Ventilating Warm Rings: Structure and Model Evaluation

WILLIAM K. DEWAR

Department of Oceanography and Supercomputer Computations Research Institute, Florida State University, Tallahassee, FL

(Manuscript received 22 May 1987, in final form 9 October 1987)

ABSTRACT

The theory of the evolution of rings under a cooling atmosphere is extended in two ways. First, the effects of stratification are studied analytically through the use of a "two and one-half" layer model. Second, model predictions are compared with observations. Qualitative support of the analytical model is also provided by a brief comparison of the analytical predictions with a numerical model.

Ring evolution is computed using the conservation of angular momentum. Idealizations in the analytical model include zero potential vorticity in the upper layer and an infinitely deep and resting third layer. The results from the analytical model, which is based on a crude representation of fluid thermodynamics, and a continuously stratified numerical model with an active mixed layer agree qualitatively. Further, both models yield predictions of main thermocline deepening under warm rings which are consistent with field observations. This agreement supports the idea that the response of warm rings to cooling is governed by Rossby adjustmentlike mechanics.

1. Introduction

It is now recognized that warm core Gulf Stream rings lose significant amounts of heat to the atmosphere and that this heat loss can cause a major modification of ring density structure. Consider for example the life history of warm ring 82B, i.e., the ring that was the focus of the recent Warm Core Rings Experiment (Evans et al., 1985; Joyce, 1985). Warm ring 82B formed in late February 1982 and from mid-March to mid-April, was observed to cool by 2°C. Further, the mixed layers in the core of 82B were observed to deepen from 325 to 425 m (Schmitt and Olson, 1985). It is clear that atmospheric exchange was responsible for these modifications.

Evans et al. (1985) suggest that the heat loss to the atmosphere from 82B occurred in two stages. The first stage was characterized by a nearly constant heat flux from the ring to the atmosphere of O(400 W m^{-2}). This flux was associated with the appearance over the ring of the relatively cold wintertime slope water atmosphere and persisted for most of the March to April period. The second stage of the heat loss coincided with the passage over the ring of a cold wintertime storm. This stage lasted only a few days but was characterized by sizeable heat losses. Schmitt and Olson (1985) estimate heat fluxes from 82B during the storm in excess of 1500 W m^{-2}.

Corresponding author address: Professor William K. Dewar, Dept. of Oceanography, Florida State University, Tallahassee, FL 32306-3048.

Another example of strong heat exchange between warm rings and the atmosphere was provided by Joyce and Stalcup (1985), who visited warm ring 82I during January, 1983. Two cold storms moved across 82I during their field effort. The second storm was decidedly more intense than the first, and Joyce and Stalcup estimate heat fluxes from 82I during that storm of O(800 W m^{-2}). They also observed a deepening of the mixed layer in 82I from 50 m to 190 m, presumably as a result of convection.

Deep thermostads have also been observed in other warm Gulf Stream rings (Joyce and Stalcup, 1985) and, for that matter, in warm rings found in other parts of the world ocean. Hata (1974) discussed a warm core Kuroshio ring with 500 m thick isothermal layers and Cresswell (1981) documented two warm eddies detached from the East Australia current, each with thick thermostads. These observations suggest that buoyancy loss to the atmosphere is a typical component of warm ring evolution.

Associated with these heat losses is a major, forced modification of the ring density field. The ring must, of course, adjust to this. Joyce and Stalcup (1985) performed XBT surveys of 82I before and after the cold storms. Based on these data, they argued that the permanent thermocline underneath the mixed layer in 82I deepened at an average rate of 1 m day^{-1} during the storms, or equivalently experienced a net downward displacement of roughly 12 m. They also discussed some indirect evidence of an outward 10 km displacement of fluid under the ring.

Similar qualitative changes in the distribution of the 10°C isotherm under warm ring 82B have been pointed

out by Olson et al. (1985). It is important to note that the 10°C surface was always beneath the mixed layer in warm ring 82B. During the period of active ventilation of this ring (i.e., from March to April), the 10°C isotherm at ring center deepened roughly 25 m. Indeed, the 10°C isotherm inside a radius of 60 km was everywhere deeper in April than in March. Outside of 60 km, however, the 10°C surface was observed to shift upward between March and April, possibly as a result of ventilation.

These comparisons suggest crudely that the secondary, radial-vertical flow in 82B during early 1982 was downward and outward at ring center, and upward and inward near the ring edge. One infers a similar circulation in warm ring 82I from the observations of Joyce and Stalcup (1985). Further, the sense of the observed circulation is opposite to that which would be driven by friction (i.e., the isotherms become steeper, rather than flatter).

In the present paper, models of cooling rings are examined in order to provide a possible explanation for the above observations. Prior modeling studies on rings have focussed on the evolution of isolated and conservative ring systems (Flierl, 1979, 1984a,b; Killworth, 1983; Nof, 1981, 1983, 1985) and have provided valuable models of ring propagation and adiabatic structure. Among the first attempts to model rings which exchanged heat with the atmosphere were those by Schmitt and Olson (1985), who examined mixed layer budgets in warm ring 82B, and Dewar (1986a), who studied surface temperature evolution in warm and cold rings. Both of these studies focussed on mixed layer dynamics and assumed that the ring was passive. Their results indicate that surface evolution in rings is primarily one-dimensional and dominated by the atmosphere.

In a more recent paper (Dewar, 1987), two-layer f-plane models of active rings under cooling atmospheres were examined. It was demonstrated that when cooled, rings develop radially inward flows at the surface and compensating outward flows at depth. Some aspects of the time dependent evolution of cooling rings were examined by computing ring structure as a function of net heat loss. Analytical "burst cooling" solutions corresponding to small heat loss were obtained and structural tendencies were computed. These solutions were used to examine the energetics of the system.

The mechanism involved in Dewar (1987) is Rossby adjustment; cooling upsets the initial force balance in the ring by inducing a relative low pressure at ring center. As the surface flow accelerates inward, a relative high pressure develops at depth and accelerates the deep fluid radially outward. The Coriolis acceleration acting on these radial mass shifts alters the swirl velocity and the system relaxes to a new balanced state.

The calculations in Dewar (1987) are extended in the present paper with a view towards examining the effects of stratification and evaluating the theory using data. In the next section, stratification is introduced by studying a three layer model with a resting lower layer. This system can be reduced to a set of simultaneous algebraic equations. Analytical solutions of this set can be obtained for small heat extractions and numerical solutions can be obtained for arbitrary heat extractions. In section 3, a numerical model is presented which employs continuous stratification and mixed layer physics. A run modeled loosely on warm ring 82B is described and qualitatively compared to the analytical solutions. Finally, the models are compared in detail with the observations of Joyce and Stalcup (1985). The agreement between the theory and the observations is encouraging.

Chapman and Nof (1988) have recently discussed an analytical model of the cooling and sinking of warm core rings. They argue that strong ventilation can bring fluid from under a warm ring to the surface and suggest this as a mechanism for the production of spiral streamers. The analytical part of the present study and the Chapman and Nof study are similar: both compute the evolution of "two and one-half" layer ring models under a cooling atmosphere. There are, however, several notable differences. For example, cooling is handled in quite different ways, and different formulations of the ring initial states are considered. The solution methods in this paper are also distinct from those of Chapman and Nof. Further, Chapman and Nof neither performed numerical calculations nor compared model predictions with data in the manner done here. Nonetheless, it is comforting to note that the models yield consistent predictions where overlap exists.

2. Analytical stratified models

a. Model development

Consider the two and one-half layer model in Fig. 1. The ocean will be modeled as Boussinesq and inviscid, and an f-plane will be used. Furthermore, the symmetry of rings will be exploited by employing a cylindrical coordinate system centered on the ring and neglecting azimuthal derivatives. Under these assumptions, the equations governing the motion in each layer are

$$u_{it} + u_i u_{ir} + w_i u_{iz} - \frac{v_i^2}{r} - f v_i = -P_{ir} \tag{1a}$$

$$v_{it} + u_i v_{ir} + w_i v_{iz} + \frac{u_i v_i}{r} + f u_i = 0 \tag{1b}$$

$$w_{it} + u_i w_{ir} + w_i w_{iz} = -P_{iz} - \rho_i g \tag{1c}$$

$$h_{it} + \frac{\partial}{\partial r}\left|\int u_i dz\right| = (-1)^{(i+1)} S \tag{1d}$$

where the subscript i obtains the values 1 and 2, and denotes the upper and lower layer respectively; u_i, v_i and w_i denote radial, azimuthal and vertical velocity,

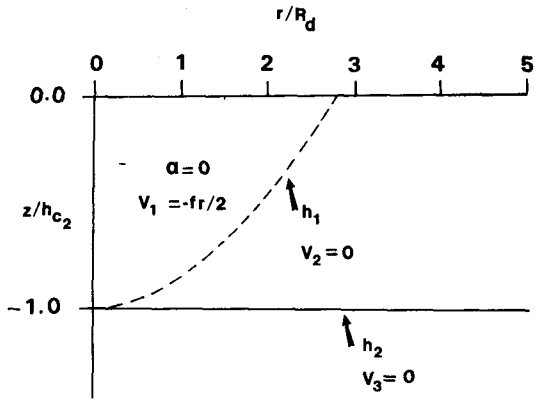

FIG. 1. A two and one-half layer model. Upper layer variables are denoted by the subscript "1" and lower layer variables by the subscript "2". Depth h_1 is of the upper interface and h_2 the depth of the second interface. The upper bowl is characterized by zero angular momentum ($\alpha = 0$), and the lower layer is initially at rest. The deepest layer is assumed to always be at rest. The model state at $t = 0$ is shown. Initially, the upper layer interface is parabolic, the second interface is flat and the interfaces meet at $r = 0$ (i.e., $h_{c_1} = h_1\ (r = 0) = h_2\ (r = 0) = h_{c_2}$).

h_i denotes thickness, P_i pressure and ρ_i density. The vertical integral is over the ith layer. The radial and vertical coordinates are r and z, and t denotes time. The third layer in this model will be taken as very deep and, therefore, stagnant. The two density defects, associated with the two interfaces, will be assigned identical values and denoted by g'.

b. *Fluid thermodynamics*

The objective of the present study is to examine the effects of heat loss on a warm ring. In order to use a layered formalism to examine such a problem, it is necessary to model the effects of cooling in a manner consistent with a layered model. The layered constraint will be maintained in the present problem by requiring the fluid to exist only in the three initial density states. Heat losses from the upper layer will be balanced entirely by converting upper layer warm fluid to cold second layer fluid. The volume of fluid converted will be that necessary to balance the heat budget.

This fluid response to cooling is reflected in the continuity equation (1e) by the inclusion of a cross-interfacial velocity, here denoted by S. If the heat flux from the ocean to the atmosphere is denoted by F, $S = -F/g'$. Positive F denotes a heat loss from the ocean. According to the model thermodynamics, such a heat flux would be balanced by a conversion of warm water to cold water and would induce a tendency for the upper layer to grow thinner. Note that a positive F is consistent with a negative S, which in turn adds a negative tendency to h_{1t}. The second layer receives fluid during the conversion and grows thicker (i.e., $h_{2t} > 0$). Note that this is reflected in (1e) if $i = 2$. Analogous buoyantly driven cross-interfacial mass fluxes have been used in several recent ventilated thermocline studies (Dewar, 1986b; Luyten, Stommel and Wunsch, 1986; Pedlosky, 1986) and are a convenient way of including diabatic effects in layered models.

It was demonstrated in Dewar (1987) that, given the above fluid response to cooling, the mixing stresses in the momentum equations associated with convection vanish. The reason for this is that upper layer warm fluid is released to the lower layer as a result of cooling. The upper layer therefore entrains no anomalous momentum from the deep fluid, and, if surface wind stress is ignored, experiences no net stress. It is therefore consistent within this model to use purely inviscid momentum equations, while retaining heat loss in the density equation. (Adamec and Elsberry, 1985, on the other hand, discuss the sensitivity of results in other types of models to viscosity.)

Equations similar to (1) have been used in past studies of Gulf Stream rings (Csanady, 1979; Flierl, 1979, 1984a,b; Nof, 1981, 1983, 1985). One novel aspect of the present analysis is that the full vertical momentum equation has been retained, as opposed to the hydrostatic balance. This is done to be as general as possible and reflects that the results in this paper do not depend upon the flow being hydrostatic at all times. This is important because the adjustment of rings to cooling will probably involve internal waves and is therefore potentially nonhydrostatic. Under these conditions, the conservation of the usual oceanographic approximation to potential vorticity is not guaranteed.

c. *Parametric constraints*

The inclusion of the quantity S in the f-plane equations assumes implicitly that heating and cooling are "stronger" effects than beta. Dewar (1987) argued by means of a scaling analysis that this holds true in rings for surface heat fluxes on the order of 1000 W m^{-2}. Since such heat fluxes are typical during cold air outbreaks over rings, the theory discussed in this paper applies most readily to the modification of rings caused by cold storms.

Equation (1b) can be rewritten in the form:

$$\alpha_t + u\alpha_r + w\alpha_z = 0 \qquad (2)$$

where $\alpha = rv + fr^2/2$ and is readily identified as the total angular momentum of a fluid parcel. Equation (2) states that angular momentum is conserved by fluid parcels. Note that the conservation of α can be demonstrated from (1b) alone, and therefore holds in the presence of nonhydrostatic phenomena, diabatic effects and arbitrary density distributions.

d. *Initial-state calculations*

The evolution of cooling rings will be computed by "turning on" the quantity S for some finite time interval. If the initial ring state is assumed to be steady

prior to cooling, it can be demonstrated that both the radial and vertical velocities must vanish (Dewar, 1987). The equations governing initial ring structure therefore reduce to

$$\frac{v_i^2}{r} + fv_i = (P_i)_r \tag{3a}$$

$$P_{iz} = -\rho_i g \tag{3b}$$

i.e., the cyclostrophic and hydrostatic balances. It is necessary to supplement the above equations with additional constraints to completely determine the initial ring structure. In the present problem, these constraints will be taken as zero angular momentum in the upper layer and vanishing swirl velocity in the second and third layers.

Zero angular momentum is equivalent to zero potential vorticity and is a convenient artifice in the analytical study of rings (Flierl, 1979, 1984b). This convenience is clearly the primary reason for examining zero angular momentum eddies. On the other hand, Kunze (1986) observed relative vorticities in warm ring 82I of $-f/2$, while the relative vorticity in a zero angular momentum eddy is $-f$. This agreement in the magnitude of observed and predicted vorticity encourages comparisons between model predictions and observations of ring response to cooling.

Equations (3) can be solved to yield the initial ring structure:

$$h_1 = h_{c_1}\left(1 - \frac{f^2r^2}{8g'h_{c_1}}\right) \tag{4a}$$

$$h_1 = h_{c_2} \tag{4b}$$

$$v_1 = -fr/2 \tag{4c}$$

$$v_2 = 0 \tag{4d}$$

where h_1 and h_2 are the depths of the upper and second interfaces, respectively, h_{c_1} is the maximum upper layer depth and h_{c_2} is the maximum second layer depth. For convenience, we will assume $h_{c_1} = h_{c_2}$. The upper layer is parabolic and outcrops at a radius of $2\sqrt{2}R_d$ (where $R_d = (g'h_{c_1})^{1/2}/f$). The lower interface is flat and the third layer is, of course, stagnant. This structure is shown in Fig. 1.

e. *Adjustment calculations*

Now suppose the ring in Fig. 1 loses heat to the atmosphere. During the cooling phase, the structure of the ring will be highly time dependent and complicated. After the cooling has stopped, however, the ring will eventually settle into a new steady state. The density field will have been altered by the cooling and the new velocity and pressure fields will reflect this. The remainder of this section will be devoted to computing these fields as a function of the net heat loss from the ring. Cooling in this model converts warm water to cool water, so the net heat loss will result in a reduction of upper layer volume. The volume of converted warm water will be denoted by δV and will be used as a measure of heat loss.

Crudely speaking, cooling in this model is envisioned as occurring in a series of high intensity bursts, separated sufficiently in time ($\sim$1 day) so that the ring can relax to a new steady state. The effects on the ring heat anomaly are cumulative: as more cooling events occur, δV grows larger. To the extent that this is a reasonable idealization of rings in the field, the dependence of ring structure on δV can be viewed as a rough indicator of the time dependent evolution of ventilating rings. The observations of warm ring 82B and other rings suggest that strong cooling events are indeed an important component in the ventilation of rings. On the other hand, the longer term, weaker background cooling which was also observed to affect 82B is missing.

After cooling, the steady ring structure will again be governed by (3) or equivalently, exploiting the hydrostatic balance, by

$$\frac{v_1^2}{r} + fv_1 = g'(h_1 + h_2)_r \tag{5a}$$

$$\frac{v_2^2}{r} + fv_2 = g'h_{2r}. \tag{5b}$$

Note that these equations apply even if the intervening time dependent flow is not hydrostatic.

The upper layer in the final state will consist of zero angular momentum fluid; therefore, $v_1 = -f/2r$ and (5a) can be integrated to yield:

$$h_1 + h_2 = \frac{-f^2r^2}{8g'} + C \tag{6}$$

where C is a constant to be determined.

The solution of (5b) is more complicated and proceeds in a series of steps. First, note it is necessary to consider four regions in the second layer of the adjusted state (see Fig. 2). The innermost region (I) is characterized by $\alpha = 0$ and extends from $r = 0$ to $r = r_\alpha$. The fluid in this region was located initially in the upper layer and released to the lower layer by cooling. Reversals in the radial gradients of angular momentum in a symmetric vortex are dynamically unstable (see Charney, 1973, for a discussion). Therefore, the zero angular momentum fluid must collect at ring center if the resulting profile is to be stable (and hence steady).

Region II consists of lower layer fluid which has been displaced radially outward by the formation of region I. The angular momentum distribution in region II is not constant: rather, it is a strong function of position and must be computed as part of the solution. Region II extends from r_α to r_∂, where r_∂ is the outcrop radius of h_1 (i.e., $h_1(r_\partial) = 0$).

Region III consists of second layer fluid which was initially under the ring but which has surfaced in the

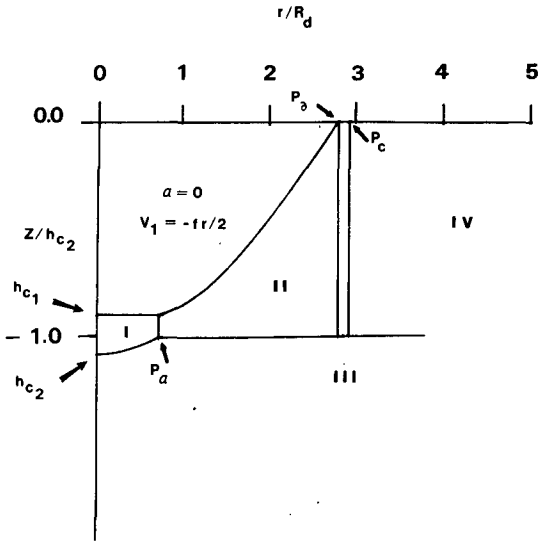

FIG. 2. The lower layer of a cooled ring divides naturally into the four indicated regions. The inner region (I) contains zero angular momentum fluid and extends to radius r_α ($r_\alpha^2/2 = P_\alpha$). Region II extends from r_α to the upper layer outcrop. Region III extends from the outcrop to the location of the fluid column which was initially at $2\sqrt{2}R_d$. This position is denoted r_c ($r_c^2/2 = P_c$). Region IV extends from r_c to ∞.

final state. Region III extends from r_∂ to r_c, where r_c is the final location of the fluid column located initially at $2\sqrt{2}R_d$.

Region IV consists of lower layer fluid which was initially outside of the ring. This region extends from r_c to ∞.

The constraint contained in (6) applies in region I and II only (i.e., where $h_1 \neq 0$). Eq. (5b) applies in all four lower layer regions.

At this point, it is convenient to define the new variables $p = r^2/2$ and $q = r_i^2/2$. Here p is simply a quadratic function of r, the radial coordinate in the final state. The quantity r_i in the definition of q denotes the initial location of a fluid column, thus $r_i(r)$ is the initial location of a fluid column which in the final state is located at r. In the following solutions, the relationship between the initial and final locations of a fluid column will be found by expressing q as a function of p.

1) THERMOCLINE STRUCTURE IN I

Differencing (5a) and (5b) yields an equation for h_1:

$$\frac{v_1^2 - v_2^2}{r} + f(v_1 - v_2) = g'h_{1r}. \tag{7}$$

Since $\alpha = 0$ in I for both upper and lower layer fluid parcels, h_1 must be a constant, thus

$$h_1 = h_{10} \quad 0 < p < P_\alpha \tag{8}$$

where $P_\alpha = r_\alpha^2/2$. Substituting (8) in (6) yields

$$h_2 = -\frac{f^2}{4g'}p + h_{20} \tag{9}$$

where h_{20} is the value of h_2 at $p = 0$ and is an unknown.

2) THERMOCLINE STRUCTURE IN II

The structure in region II is slightly more complicated. The angular momentum distribution in II can be written as fq, since v_2 vanished in the initial state. Equation (5b) can therefore be written in II as

$$\frac{f^2}{4}\frac{q^2}{p^2} - \frac{f^2}{4} = g'(h_2)_p \tag{10}$$

to yield one relation between h_2 and q.

A two step argument can be used to obtain a second constraint. It is first noted that the fluid is Boussinesq; therefore, if V is the volume of a piece of fluid enclosed by a material surface, $dV/dt = 0$. Second, since angular momentum is conserved by fluid parcels, sheets of constant angular momentum define material surfaces. Therefore,

$$V_\alpha = \int_0^{2\pi}\int_{-h_2}^{0}\int_0^{r_\alpha} rdrdzd\theta,$$

where $r_\alpha(Z)$ is the radial location of a particular α value, are constants of the system and can be computed from the initial conditions.

This volume constraint is expressed in region II as

$$\frac{f^2}{8g'}q^2 = \int_0^p (h_2 - h_1)dp.$$

Differentiating the above with respect to p yields

$$\frac{f^2}{8g'}\frac{\partial q^2}{\partial p} = (h_2 - h_1), \tag{11}$$

which when combined with (6) and (10) yields the governing equation in region II:

$$\frac{\partial^2}{\partial p^2}\frac{f^2}{8g'}q^2 = \frac{f^2}{2g'}\frac{q^2}{p^2} - \frac{f^2}{4g'}. \tag{12}$$

Thus

$$q^2 = p^2 + Ap^{\beta_1} + Bp^{\beta_2} \tag{13}$$

in (II), where

$$\beta_1 = \frac{1 + \sqrt{17}}{2} > 0 \quad \text{and} \quad \beta_2 = \frac{1 - \sqrt{17}}{2} < 0. \tag{14}$$

Combining (10) and (13) yields h_2, and h_1 can be computed from (6).

3) THERMOCLINE STRUCTURE IN III

The fluid in III also originated in the second layer, so (10) applies to the thermocline structure in this region. It should also be obvious that the angular momentum volume constraint appropriate to III can be

obtained by setting $h_1 = 0$ in (11). These two constraints can be combined to yield the single governing equation:

$$\frac{\partial^2}{\partial p^2} q^2 = 2\frac{q^2}{p^2} - 2 \tag{15}$$

whose solution is

$$q^2 = Kp^2 + lp^{-1} - 2p^2 \ln(p)/3 \tag{16}$$

which completely describes region III.

4) THERMOCLINE STRUCTURE IN IV

It has been necessary in IV to replace the cyclostrophic balance with a geostrophic balance in order to retain analytic tractability. This amounts to neglecting the nonlinear term in (5b). The expression of geostrophy is

$$\frac{f^2}{2}\frac{(q-p)}{p} = g'(h_2)_p \tag{17}$$

while the angular momentum volume conservation constraint is

$$\frac{\partial q}{\partial p} = h_2/h_{c_2} \tag{18}$$

where h_{c_2} is the initial maximum thickness of layer 2. Combining (17) and (18) yields the governing equation:

$$\frac{\partial}{\partial p} p \frac{\partial}{\partial p} h_2 = \frac{f^2}{2g'}\left(\frac{h_2}{h_{c2}} - 1\right). \tag{19}$$

The solution for the thermocline in IV is thus

$$h_2 = h_{c_2} + DK_0(r/R_d) \tag{20}$$

where K_0 is the modified Bessel function of order zero of the second kind. [The I_0 Bessel function solution of (19) has been discarded because of its exponential behavior for large r.] In (19) R_d is defined by $(g'h_{c_2})^{1/2}/f$. For reference,

$$p = q - D(2p)^{1/2}K_1[(2p)^{1/2}/R_d] \tag{21}$$

where K_1 is the order one modified Bessel function.

f. Constraints

There are 11 unknowns in the structure solutions, namely P_α, h_{10}, h_{20}, C, P_∂, A, B, K, l, P_c and D. The conditions to be appended to the equations (8), (9), (13), (16) and (20) are continuity of q and h_2 at P_α, continuity of q and h_2 at P_∂, $h_1(P_\partial) = 0$, continuity of h_2 and q at P_c and $q(P_c) = 4R_d^2$. The two other constraints necessary to close the problem are provided by the volume constraints reflecting the net heat loss from the ring:

$$2\pi \int_0^{P_\alpha} (h_2 - h_1)dp = \delta V$$

$$2\pi h_{10}P_\alpha + 2\pi \int_{P_\alpha}^{P_\partial} h_1 dp = V_0 - \delta V.$$

If p and q are nondimensionalized by R_d^2, and h_1 and h_2 by h_{c_1}, the nondimensional initial warm water volume is found to be 4 and the following set of 11 nonlinear algebraic equations in 11 unknowns is obtained:

$$(h_{20} - h_{10})P_\alpha - \frac{1}{8}P_\alpha^2 = \delta V/2 \tag{22a}$$

$$h_{10}P_\alpha + \frac{C}{2}(P_\partial - P_\alpha) - (P_\partial^2 - P_\alpha^2)/8 - \frac{\beta_1 A}{16(\beta_1 - 1)}(P_\partial^{\beta_1} - P_\alpha^{\beta_1}) - \frac{\beta_2 B}{16(\beta_2 - 1)}(P_\partial^{\beta_2} - P_\alpha^{\beta_2}) = 2 - \delta V/2 \tag{22b}$$

$$h_{10} = \frac{C}{2} - \frac{P_\alpha}{4} - \frac{\beta_1}{16}AP_\alpha^{\beta_1 - 1} - \beta_2\frac{B}{16}P_\alpha^{\beta_2 - 1} \tag{22c}$$

$$h_{20} - \frac{P_\alpha}{4} = \frac{C}{2} + \frac{\beta_1}{16}AP_\alpha^{\beta_1 - 1} + \frac{\beta_2}{16}BP_\alpha^{\beta_2 - 1} \tag{22d}$$

$$0 = P_\alpha^2 + AP_\alpha^{\beta_1} + BP_\alpha^{\beta_2} \tag{22e}$$

$$0 = \frac{C}{2} - \frac{P_\partial}{4} - \frac{\beta_1}{16}AP_\partial^{\beta_1 - 1} - \frac{B}{16}\beta_2 P_\partial^{\beta_2 - 1} \tag{22f}$$

$$\frac{C}{2} + \frac{\beta_1}{16}AP_\partial^{\beta_1 - 1} + \frac{B}{16}\beta_2 P_\partial^{\beta_2 - 1} = \frac{K}{4}P_\partial - \frac{l}{8}P_\partial^{-2} - \frac{1}{6}P_\partial \ln P_\partial - P_\partial/12 \tag{22g}$$

$$\frac{K}{4}P_c - \frac{l}{8}P_c^{-2} - \frac{1}{6}P_c \ln P_c - P_c/12 = 1 + DK_0(\sqrt{2P_c}) \tag{22h}$$

$$P_\partial^2 + AP_\partial^{\beta_1} + BP_\partial^{\beta_2} = KP_\partial^2 + lP_\partial^{-1} - 2P_\partial^2 \ln(P_\partial)/3 \tag{22i}$$

$$16 = KP_c^2 + lP_c^{-1} - 2P_c^2 \ln(P_c)/3 \tag{22j}$$

$$4 = P_c - D(2P_c)^{1/2}K_1[(2P_c)^{1/2}] \tag{22k}$$

Note that the set $h_{01} = h_{02} = 1$, $P_\alpha = 0$, $P_\partial = P_c = 4$, $A = B = D = 0$, $C = 2$, $K = 11/9 + 2\ln(4)/3$ and $l = -128/9$ satisfies the constraints in (22) for the special case $\delta V = 0$. This will be referred to as the base solution set.

The set of simultaneous constraints in (22) are nonlinear and cannot be solved analytically for arbitrary δV. There are two special cases, however, where analytical progress towards obtaining the solution of this system can be made, namely $\delta V \ll 1$ and $\delta V = V_0$. These special cases correspond to small heat losses and complete heat loss (or "total ventilation"). The former, as we will argue shortly, is typical of heat loss caused by strong storms. Also, it is not difficult to extract the solution set of (22) numerically for any value of δV.

g. Analytical solutions for small heat withdrawal

It is expected that for small δV, the solution set of (22) should differ only slightly from the base solution set. Equation (22a) suggests corrections to h_c, h_0 and P_α of $O(\delta V)^{1/2}$ in agreement with this expectation. If this scaling for P_α is accurate, (22e) shows that the combination $AP_\alpha^{\beta_1}$ and/or $BP_\alpha^{\beta_2}$ must scale as δV. Recall that $\beta_1 > 0$, while $\beta_2 < 0$. If $AP_\alpha^{\beta_1}$ is $O(\delta V)$, A must scale as $O(\delta V^{(3-\sqrt{17})/4})$, which is large. This scaling can be rejected because it does not represent a small correction to base solution for A and, further, it induces large changes in other unknowns [cf. (22f)].

On the other hand, if $BP_\alpha^{\beta_2}$ is $O(\delta V)$, B scales as $O(\delta V^{(3+\sqrt{17})/4})$, which is small and therefore acceptable. Thus, the primary balance in (22e) involves P_α^2 and $BP_\alpha^{\beta_2}$, and it can be concluded that $AP_\alpha^{\beta_1}$ must be smaller than $O(\delta V)$. The latter result implies that the terms involving A can be neglected in both (22c) and (22d) and that the deviation of C from its base solution is at most $O(\delta V^{1/2})$.

An expansion of all variables, apart from B, in powers of $(\delta V)^{1/2}$ about the base solution is therefore substituted into (22). The expression $B_1\delta V^{(3+\sqrt{17})/4}$ is substituted for B. It is then possible to isolate a homogeneous 7×7 subsystem from (22) involving the quantities C_1, $P_{\partial,1}$, A_1, K_1, l_1, $P_{c,1}$ and D_1, where the subscript 1 denotes an $O(\delta V^{1/2})$ correction.

It can be shown that the solution for all the coefficients in this homogeneous system is zero. The equations involving the remaining four unknowns can thus be considerably simplified and solved directly. The results are:

$$P_{\alpha,1} = 2/\sqrt{4 - \beta_2 - 1}$$

$$h_{20,1} = \frac{1}{8}\left[\sqrt{4 - \beta_2 - 1} + (\sqrt{4 - \beta_2 - 1})^{-1}\right]$$

$$h_{20,1} = -h_{10,1}$$

$$B_1 = -\left(\frac{4}{4 - \beta_2 - 1}\right)^{1-\beta_2/2}$$

Approximating $\beta_2 = \dfrac{1 - \sqrt{17}}{2}$ by $-3/2$,

$$P_\alpha = 0.9(\delta V)^{1/2}$$

$$h_{20} = 1 + \frac{5}{16}(\delta V)^{1/2}$$

$$h_{10} = 1 - \frac{5}{16}(\delta V)^{1/2}$$

$$B_1 = -0.98.$$

The above approximations for h_{10} and P_α are plotted against numerically derived solutions in Fig. 3. It is clear that the approximations are acceptable at least out to $\delta V = 0.2V_0$.

The fact that the $(\delta V)^{1/2}$ corrections vanish for the remaining seven unknowns indicates that they deviate from the base solution no faster than δV. It is also true that these seven unknowns are related to the thermocline structure relatively far from ring center. The variables P_α, h_{10}, h_{20} and B are associated with structure near ring center. It is therefore evident that the largest diabatically forced structural modifications in a ring are found near ring center.

A sketch of the adjusted ring structure for $\delta V = 0.16$ is given in Fig. 4. Note that the two upper layer isotherms, which were initially touching at $p = 0$, have everywhere separated by a finite distance. Further, the perturbations to the thermocline structure decay quickly away from ring center. The azimuthal velocity profile in the lower layer (not shown) consists of $\alpha = 0$ fluid with $v = -fr/2$ out to P_α, followed by a rapid decay of v to zero.

h. Structure solutions for total ventilation

The other parameter regime in which analytical progress is possible occurs if $\delta V = V_0$. The ring in this case is said to be totally ventilated and h_{10} obviously vanishes. If the solution $P_\alpha = P_\partial$ is attempted, (22b) is satisfied and (22c) and (22f) become redundant. The constraints are therefore reduced to a 9×9 system. Explicit reference to A and B is easily eliminated and C is found to be h_{20}. Further manipulation of the resulting 6×6 system yields the coupled equations:

$$P_\alpha{}^3/9 - \frac{16}{3}P_\alpha = \frac{32}{3}P_c - \frac{8}{3}P_c^2 - \frac{\frac{8}{3}P_c^2(P_c - 4)K_0(\sqrt{2P_c})}{\sqrt{2p_c}K_1(\sqrt{2P_c})} - \frac{2}{9}P_c^3 \quad (23a)$$

$$16P_c^{-2} + \frac{2}{3}\ln(P_c) - \left(\frac{P_\alpha{}^3}{9} - \frac{16}{3}P_\alpha\right)P_c^{-3} = \frac{2}{3}\ln P_\alpha + \frac{16}{3}P_\alpha^{-2} - \frac{1}{9}. \quad (23b)$$

Additional equations specify the remaining variables, the most important of these being:

$$h_{20} = \frac{2}{P_\alpha} + \frac{P_\alpha}{8} \quad (24)$$

The solution to (23) is easily extracted numerically, and is

$$P_\alpha = 1.67 \quad (25a)$$

$$P_\partial = 3.82. \quad (25b)$$

Therefore,

$$h_{20} \approx 1.4. \quad (25c)$$

Graphs of both the thermocline and the azimuthal velocity for a totally ventilated ring are presented in Fig. 5. Note the O(1) net downward displacement of

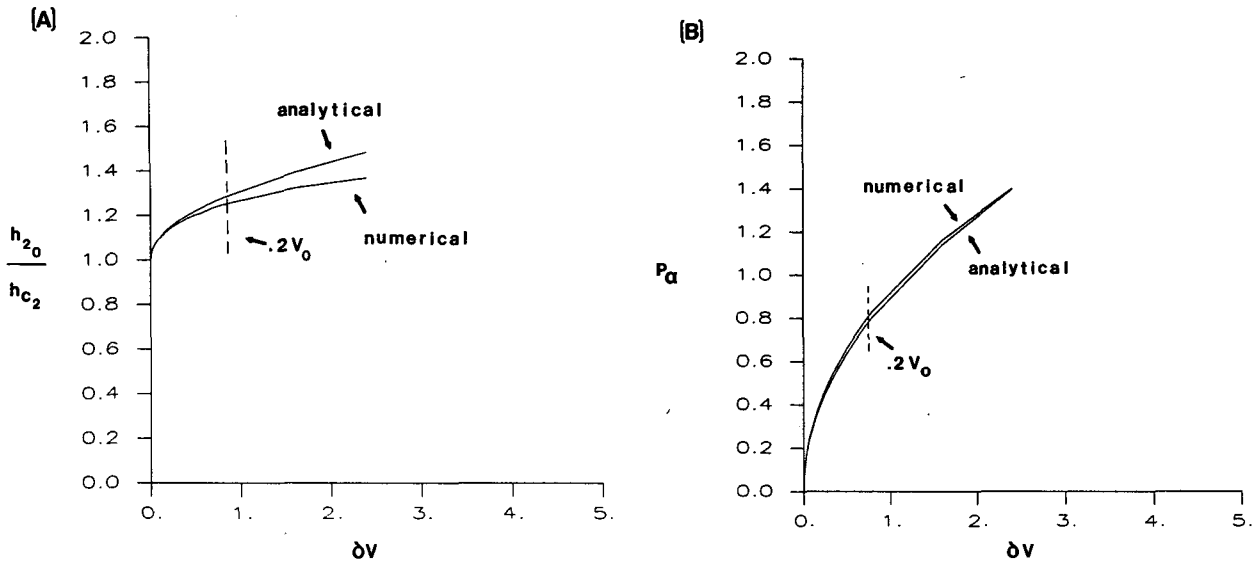

FIG. 3. The analytical small heat withdrawal approximate solutions for (a) h_{20} and (b) P_α are compared to the numerical solutions for h_{20} and P_α. The approximate solutions are accurate to out $\delta V = 0.2V_0$.

the thermocline at ring center, and that further out, the thermocline has actually become slightly shallower than its initial value. The azimuthal velocity profile consists of a linear decrease moving outward from $r = 0$ to r_α. This is followed by a rapid increase in v to a region where the velocity reverses in sign. The magnitude of the positive v value is O(10 cm s^{-1}) and is consistent with the slight inward displacement of the fluid initially at $4R_d$ to a final position of $3.82R_d$ [see (25b)]. The vertical-radial fluid circulation inferred from comparing the initial and final plots consists of a counterclockwise cell, with inward directed surface flows, relatively vigorous negative vertical velocities near ring center, radially outward deeper flows, and weak, widely distributed positive vertical velocities away from ring center.

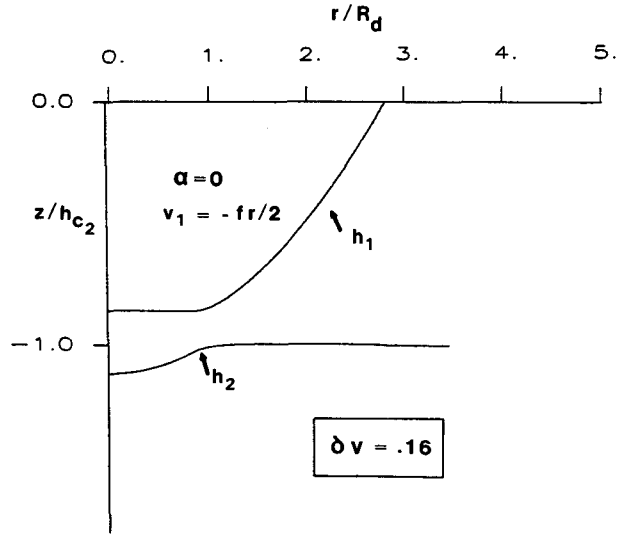

FIG. 4. Thermocline structure for $\delta V = 0.16$. The lower interface has deepened and the upper interface has risen in response to the cooling. The lower thermocline perturbation decays quickly for increasing r. The upper layer outcrop has moved inward very slightly. Note that the largest changes in the thermocline occur near ring center.

Note, the O(10 cm s^{-1}) velocities found in region IV are consistent with the geostrophic approximation employed there. The ratio of the neglected centrifugal term to the Coriolis term is $v^2/(rfv) = 0.03 \ll 1$.

The mechanisms behind the evolution of a cooling ring are closely related to those involved in Rossby adjustment. Cooling upsets the force balance in the initial vortex by affecting the vortex pressure field. Pressure imbalances then cause radial mass shifts which are, in turn, accompanied by acceleration of azimuthal velocity. The magnitude of the azimuthal velocity is governed by angular momentum conservation. Since angular momentum involves a contribution from the Coriolis parameter, and this is a dominant parameter of the system, even relatively small displacements are accompanied by large variations in swirl speed.

The radial displacements result in a final balanced state, which differs from the initial state by an amount dependent upon the net cooling. The primary difference between the present results (with a deformable lower boundary) and those of Dewar (1987) (which employed a rigid lower boundary) is that a significant fraction of the pressure and mass field adjustments can occur baroclinically. The cooled fluid tends to move inward. The radial geometry focuses this movement and magnifies it at ring center. The fluid which has not been cooled responds by shifting both outward and downward. Isotherms under the region of active convection are therefore depressed and fluid on those isotherms experiences an outward displacement. Both

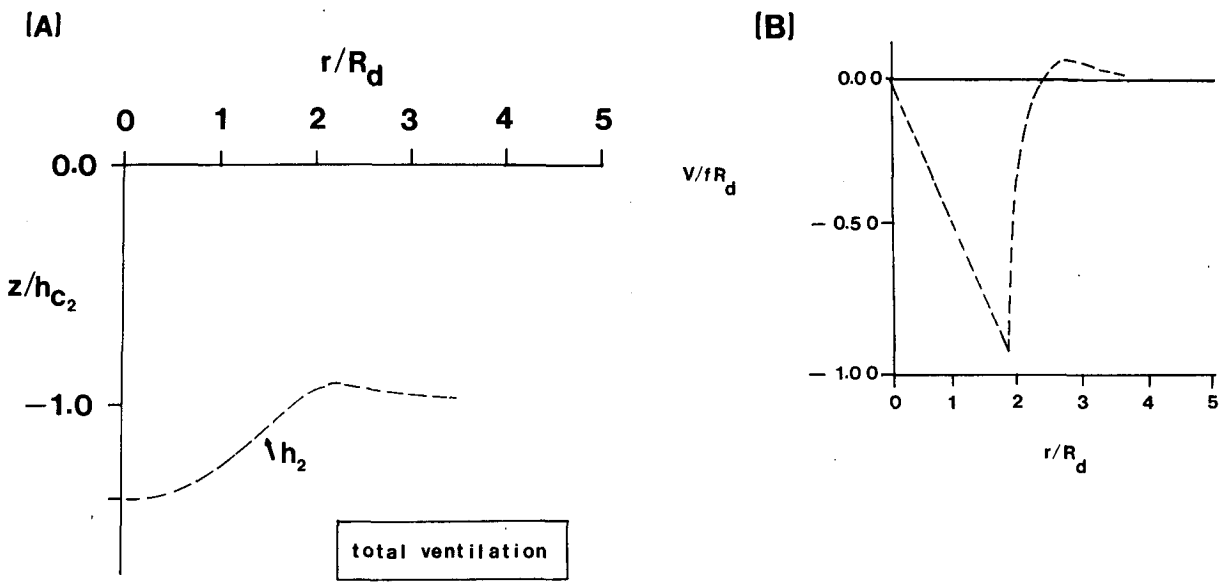

FIG. 5. Thermocline and velocity structure for a totally ventilated ring. (a) The thermocline at ring center has been depressed by an O(1) amount, while for large r the thermocline has actually risen. (b) The velocity structure is linear out to radius r_α, and then drops rapidly in magnitude. A reversal in azimuthal velocity of O(10 cm s^{-1}) is observed.

predictions seem to fit with observations, as will be discussed in section 4.

3. A numerical model of a ventilating warm ring

The calculations in the previous section have, in some sense, computed the time dependent evolution of ventilating rings by considering the dependence of the ring structure on the parameter δV, the volume of converted water. A more direct method of computing the time dependent response of rings to ventilation is to solve the problem numerically. To this end, I have begun experimentation with a coupled mixed layer/interior numerical model of an f-plane ring. The derivation of the model is given in appendix A. In summary, the governing equations are

$$\alpha_t + \frac{1}{r} J(\psi, \alpha) = 0 \tag{26a}$$

$$\rho_t + \frac{1}{r} J(\psi, \rho) = (\overline{-w'\rho'})_z \tag{26b}$$

$$gr^3\left[\frac{1}{r} J(\psi, \rho)\right]_r + \left[\frac{1}{r} J(\psi, \alpha^2)\right]_z = -gr^3(\overline{w'\rho'})_{zr} \tag{26c}$$

where $\alpha = rv + fr^2/2$ is angular momentum (as before), ρ density and ψ a vertical-radial streamfunction defined by

$$\psi_r = rw$$

$$\psi_z = -ru.$$

The notation $J(A, B)$ denotes the usual Jacobian operator

$$J(A, B) = A_r B_z - A_z B_r.$$

The model conserves angular momentum (26a). The density flux divergence term, $(\overline{-w'\rho'})_z$, in (26b) is computed according to the mixed-layer model proposed in Dewar (1986a). This model responds to cooling by convective adjustment and qualitatively reproduces the seasonal sea surface temperature evolution of both warm and cold rings. Cooling upsets the density field, and therefore the pressure field, of a ring. Fluid parcels then shift position in response to the unbalanced forces. The required motion is represented by the streamfunction ψ. The advantages of the numerical model in (26) over the analytical model of section 2 are that it is continuously stratified and incorporates an active mixed layer model.

An example of the evolution computed by the numerical model is shown in Fig. 6. The density initial condition for this run is shown in (a) and was modeled loosely after warm ring 82B (e.g., see Schmitt and Olson, 1985). Air temperatures over the ring were begun at 0°C and cycled at an annual frequency with a peak to trough amplitude of 20°C. This amplitude is characteristic of the seasonal variation of atmospheric temperatures in the slope water. Initializing the experiment with the coldest air temperatures was meant as a crude model of the late February formation date of 82B. The maximum surface heat fluxes in this run were O(600 W m^{-2}), significantly less than the maximum fluxes from 82B and 82I, but comparable to their average heat fluxes.

Shown in Fig. 6 are the streamfunction and temperature fields of the ring after 40 days (b) and at the

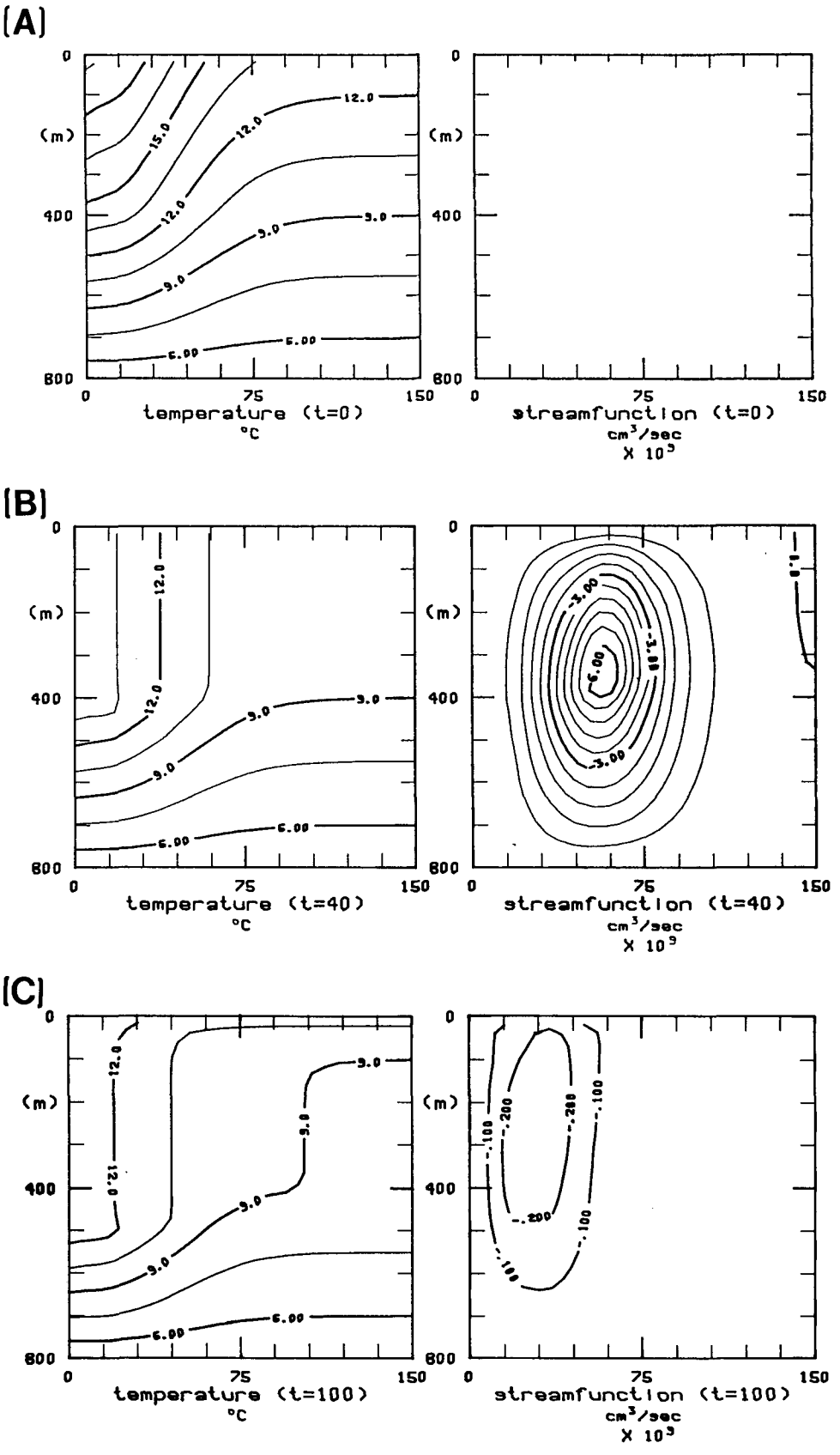

FIG. 6. Examples of numerically computed ring evolution. The initial density field is shown in (a), and was chosen to loosely model the isotherm structure in warm ring 82B. The thermocline structure and radial–vertical streamfunction at 40 days is shown in (b). The surface flow is inward and the deep flow is outward. Vertical velocities are O(-1 m day^{-1}) at ring center and substantially weaker further out. The density structure and streamfunction at the onset of restratification are shown in (c). Note that restratification rapidly damps the vertical radial flow.

onset of restratification (c). The streamfunction obtains a local minimum at depth, consistent with radially inward flows at the surface and outward flows at depth. The magnitudes of these radial flows are O(0.1 cm s^{-1}). The isotherms under the central warm ring mixed layer clearly deepen. The magnitude of the vertical velocities can be computed from the streamfunction and at ring center are O(−1 m day^{-1}). Further out, the sense of w reverses and its magnitude is smaller than near ring center. The streamfunction structure is strongly confined to the vicinity of the ring and the point of the streamfunction extremum tracks the maximum mixed-layer depth. Finally, note in (c) that the onset of springtime restratification effectively kills the vertical–radial circulation.

The one aspect of the analytical model for which there is no clear analog in the numerical model is the behavior of the upper isotherm. The analytical model predicts this interface will rise, while "mixing" in the numerical model keeps all temperature surfaces in the mixed layer purely vertical. Aside from this point, the overall tendencies of the isotherms under the mixed layer, the sense of the vertical–radial circulation and the magnitudes of the tendencies are in general agreement between the analytical and numerical models. One therefore concludes that the motion of the upper interface in the analytical model reflects the cross interfacial mass flux parameterization of cooling, which is the least believable aspect of the model. Other aspects of the analytical model, such as the motion of the second interface, are sensitive to heat withdrawal in the same manner as the numerical model. Comparisons between the analytical model predictions and observations (discussed in the next section) will therefore be confined to the fluid beneath the region of active cooling.

4. Discussion

The parameter assumptions justifying the f-plane analysis contained herein are characteristic of strong episodic cooling events. The best observations of ring-scale response to such events are those of Joyce and Stalcup (1985) in warm ring 82I. The small heat loss analytical solutions presented in section 2 are here applied to 82I for comparison with the observations.

Joyce and Stalcup suggest, on the basis of XBT transects, that 82I had a relatively weak baroclinic structure; for example, the depression of the 10°C isotherm is roughly 100 m and is 3 to 5 times smaller than for many other rings. Examination of the ring structure in Joyce and Stalcup (their Fig. 6) suggests the "bowl" of warm ring water is contained within the upper 200 m. Certainly this is the scale of the convective overturning caused by the two observed cooling events. I will therefore assign the value of 200 m to the maximum initial model upper layer thickness. The initial model ring radius is thus $2\sqrt{2}R_d \sim 40$ km, not much different from the ~30 km radius of the observed velocity maximum in 82I.

Joyce and Stalcup estimate a net heat loss from ring center to the atmosphere of 0.35×10^9 J m^{-2} because of the passage of the two cold air outbreaks. Assuming this heat loss falls off linearly to the ring boundary, a net heat loss over the ring of 5.8×10^{17} J is realized. It is admittedly not obvious how this heat loss should be converted to a measure of volume loss for comparison with the analytical results, but here the model upper layer is equated with the heat anomaly of the ring. Examining the XBT data presented in Joyce and Stalcup (their Fig. 7) suggests that 82I is ~3°C warmer than its surroundings. This gives 82I a net heat anomaly of 5.7×10^{18} J. It therefore appears that O(10%) of the heat anomaly in 82I was lost during the two cooling events. Using this estimate to determine the volume loss parameter yields a value of $\delta V = 0.4$ (recall that $V = 4$ nondimensionally).

From the analytical results in section 2, a net depression of

$$\delta h = \frac{5}{16}(\delta V)^{1/2} h_{1c} \approx 40 \text{ m}$$

for the thermocline under ring center is computed. Joyce and Stalcup (1985) argue that the thermocline under 82I deepened at an average rate of 1 m day^{-1} during the period of intense cooling. This represents a net downward thermocline displacement of 12 m. Given the inherent uncertainty in the calculation of δV and other model assumptions, the comparison of these observations with the model prediction of 40 m is encouraging. At the least, theory suggests that for reasonable heat extractions, the net effect at ring center will be tens of meters. (As further evidence of this order of magnitude, Olson et al., 1985, found that the 10°C isotherm under warm ring 82B experienced a downward displacement of 25 m from March to April. It is also clear that this was a period of active ventilation in 82B.)

Joyce and Stalcup (1985) also discuss the outward movement of an anomalous water mass at a depth of 300–350 m in 82I. This lateral displacement moved the anomaly from their 0–20 km averaging bin to their 20–40 km averaging bin, and is suggestive of an O(10 km) displacement. According to the analytical results, one predicts net outward displacements under 82I of

$$\delta r \approx (1.4)(\delta V)^{1/4} R_d = 15 \text{ km}.$$

Again the model predictions agree in magnitude with the suggestions from data.

The above predictions for δr and δh both reflect the special choice $h_{c_1} = h_{c_2}$. Given model shortcomings (i.e., 2½ layers, $\alpha = 0$, cooling parameterization), the useful aspect of these predictions is their order of magnitude ($\delta r \sim 10$ km, $\delta h \sim 10$ m) rather than their absolute value. This order of magnitude agreement between predictions and observations suggests that the Rossby adjustmentlike mechanism, which is at the heart of the present calculations, is a reasonable model of the physics in a ventilating ring. The calculations

also emphasize that the effects of ventilation are amplified at ring center both in velocity and the modification of the thermocline. Future observational programs might be well advised to monitor the evolution of rings near their center.

5. Conclusions

In this paper, f-plane models of rings evolving under cooling atmospheres have been considered. The response of the rings is governed by a Rossby adjustment type process. Cooling a ring alters its density distribution, which in turn upsets the ring pressure field. The ring then adjusts its mass and momentum fields so as to return to a cyclostrophic state. An important, conserved quantity in this process is angular momentum. Potential vorticity is not conserved because of diabatic effects. Detailed calculations of ring response have been made using two and one-half layer models with crude parameterizations of convection. Some analytical progress on the time dependent ring evolution has also been made by considering the dependence of the ring structure on the parameter δV, which measures the extent of the cooling. Comparisons of the analytical calculations with some numerical calculations yields qualitative support for the analytical model. For example, both the numerical and analytical models predict main thermocline deepening rates of ~ 1 m day^{-1} for relatively strong cooling.

Model predictions and the field observations of warm ring 82I made by Joyce and Stalcup (1985) compare favorably in magnitude. The main thermocline under 82I was observed to deepen by 10–15 m as a result of two cold air outbreaks. The model predictions, when tuned to 82I, suggest a 40 m deepening of the thermocline which, in view of the uncertainties, is taken to be encouraging. The model also predicts an outward shift of O(10 km) for the fluid under warm ring 82I. There are hints in the Joyce and Stalcup data that such a shift occurred.

The present work depends to a certain extent on two assumptions; namely, the assumption of zero angular momentum in the warm ring, and the warm-to-cold water parameterization of convection. To this end, work is in progress on models which relax these constraints and further experimentation with the numerical model, introduced in the Appendix, is planned. Regarding the zero angular momentum assumption, it should be noted that the present formalism will apply to more general angular momentum distributions. The algebra becomes somewhat more complicated, however, and it appears that numerical solutions of the governing equations are required.

Acknowledgments. This work has benefitted from conversations with Drs. John Bane and Doron Nof. Rick Chapman, who has worked on a closely related subject, is also thanked for his insight. My research is sponsored by NSF Grant OCE 8415475 and ONR Grant N001487G0209. The costs of manuscript preparation were covered by a grant from the Committee on Research and Creativity of the Florida State University. Pat Klein typed the manuscript and is thanked for her patience.

APPENDIX A

A Numerical Model of a Ventilating Warm Ring

Numerical Model Development

The equations of motion for a symmetric, continuously stratified, Boussinesq, f-plane ring are

$$u_t + uu_r + wu_z - \frac{v^2}{r} - fv = -P_r \tag{A1}$$

$$v_t + uv_r + wv_z + \frac{uv}{r} + fu = 0 \tag{A2}$$

$$w_t + uw_r + ww_z = -P_z - \rho g \tag{A3}$$

$$\rho_t + u\rho_r + w\rho_z = -(\overline{w'\rho'})_z \tag{A4}$$

$$(ru)_r + (rw)_z = 0 \tag{A5}$$

where the notation is standard. Comparing the nonlinear and local acceleration terms in (A1) to the cyclostrophic terms yields ratios like:

$$\frac{u_t}{fv} = \mathrm{O}\left(\frac{U}{V}\frac{1}{fT}\right)$$

$$\frac{uu_r}{fv} = \mathrm{O}\left[\left(\frac{U}{V}\right)^2 \frac{V}{fL}\right]$$

where U is a scale estimate of the radial flow, V a scale estimate of the swirl flow and L is a ring length scale; V/fL is the Rossby number and can be O(1). On the other hand, it is expected that the ratio U/V is small, and further that the time scale of the ring response is not shorter than a pendulum day. Therefore $1/fT$ is at best O(1), and the above ratios are seen to be small. The radial momentum equation is thus approximated by the cyclostrophic balance:

$$\frac{v^2}{r} + fv = P_r.$$

Similar scaling analysis, when applied to the azimuthal momentum and density equations, suggests that all terms are the same order of magnitude. Of course, the azimuthal momentum equation can be manipulated into the form

$$\frac{d}{dt}\alpha = 0$$

where $\alpha = rv + fr^2/2$. For simplicity, the vertical momentum equation is approximated by the hydrostatic balance and a vertical–radial streamfunction ψ, defined by

$$\psi_r = rw \tag{A6}$$

$$\psi_z = -ru \tag{A7}$$

is used to solve the continuity equation (A5).

The numerical model equations are thus:

$$\alpha_t + \frac{1}{r} J(\psi, \alpha) = 0 \tag{A8}$$

$$\rho_t + \frac{1}{r} J(\psi, \rho) = -(\overline{w'\rho'})_z \tag{A9}$$

$$2\alpha\alpha_z = -r^3 g\rho_r \tag{A10}$$

where (A10) is analogous to the thermal wind constraint. Equations similar to (A8)–(A10) have been examined by Flierl and Mied (1985) in a study of rings and in the context of hurricanes by Hack and Schubert (1986 and references therein). The most computationally convenient form of (A8)–(A10) is obtained by using (A10) to eliminate α_t and ρ_t from (A8) and (A9). The result is a diagnostic and elliptic equation for ψ. Furthermore, if (A8)–(A10) are formally transformed from the (r, z, t) coordinate system to a new (r', z', t') system, where the coordinates are defined by

$$r' = r^2/2$$

$$z' = z$$

$$t' = t,$$

the equations take the convenient form:

$$\alpha_t + J'(\psi, \alpha) = 0 \tag{A11}$$

$$\rho_t + J'(\psi, \rho) = -(w'\rho')_{z'} \tag{A12}$$

$$[J'(\psi, \alpha^2)]_{z'} + 4gr'^2[J'(\psi, \rho)]_{r'} = -4gr'^2(w'\rho')_{zr'}. \tag{A13}$$

The Jacobian in the above equations is based on r' and z'; i.e.:

$$J'(A, B) = A_{r'}B_{z'} - A_{z'}B_{r'}$$

The advantage of the "warped" (r', z', t') system is that it makes the Jacobians look "Cartesian." Standard Arakawa finite difference formulations can therefore be employed.

The Reynolds term, $(\overline{w'\rho'})_z$, is calculated using the mixed layer model proposed in Dewar (1986a). This model responds to cooling through convective adjustment, and to heating by the formation of a 30-m deep mixed layer. Atmospheric temperature is prescribed over the ring and the sensible, latent and radiative heat fluxes are computed using a Newtonian cooling law:

$$\text{Heat flux} = \frac{(40 \text{ watts})}{(\text{m}^2\ ^\circ\text{C})} (T - T_a)$$

where T is the sea surface temperature and T_a the atmospheric temperature. Penetrative solar radiation is computed using typical double exponential parameterizations. Density is computed according to

$$\rho = \rho_0[1 - \gamma(T - T_0)]$$

where $\gamma = 2 \times 10^{-4}/^\circ\text{C}$. Dewar (1986a) has argued that such a mixed layer model accurately reproduces the seasonal sea surface temperature evolution of both warm and cold rings.

REFERENCES

Adamec, D., and R. Elsberry, 1985: Response of an intense oceanic current system to cross-stream cooling events. *J. Phys. Oceanogr.*, **15,** 273–287.

Chapman, R., and D. Nof, 1988: The cooling and sinking of warm core rings. *J. Phys. Oceanogr.*, **18,** 565–583.

Cresswell, G. R., 1981: The coalescence of two East Australia Current warm-core rings. *Sci.*, **215,** 161–164.

Csanady, G. T., 1979: The birth and death of a warm core ring. *J. Geophys. Res.*, **84,** 777–780.

Dewar, W. K., 1986a: Mixed layers in Gulf Stream rings. *Dyn. Atmos. Oceans,* **10,** 1–29.

——, 1986b: On the potential vorticity structure of weakly ventilated isopycnals: A theory of subtropical mode water maintenance. *J. Phys. Oceanogr.*, **16,** 1204–1216.

——, 1987: Ventilating warm rings; Theory and energetics. *J. Phys. Oceanogr.*, in press.

Evans, R. H., K. S. Baker, O. B. Brown and R. C. Smith, 1985: Chronology of warm core ring 82B. *J. Geophys. Res.*, **90,** 8803–8817.

Flierl, G. R., 1979: A simple model for the structure of warm and cold core rings. *J. Geophys. Res.*, **84,** 781–785.

——, 1984a: A model for the structure and motion of a warm core ring. *Aust. J. Mar. Freshwater Res.*, **35,** 9–23.

——, 1984b: Rossby wave radiation from a strongly nonlinear warm eddy. *J. Phys. Oceanogr.*, **14,** 47–58.

——, and R. P. Mied, 1985: Frictionally induced circulations and spin down of a warm-core ring. *J. Geophys. Res.*, **90,** 8917–8927.

Hack, J. J., and W. H. Schubert, 1986: Nonlinear response of atmospheric vortices to heating by organized cumulus convection. *J. Atmos. Sci.*, **43,** 1559–1573.

Hata, K., 1974: Behavior of a warm eddy detached from the Kuroshio. *J. Meteor. Res.*, **26,** 295–321.

Joyce, T. M., 1985: Gulf Stream warm-core ring collection: An introduction. *J. Geophys. Res.*, **90,** 8801–8802.

——, and M. C. Stalcup, 1985: Wintertime convection in a Gulf Stream warm-core ring. *J. Phys. Oceanogr.*, **15,** 1032–1042.

Killworth, P. D., 1983: On the motion of isolated lenses on a beta-plane. *J. Phys. Oceanogr.*, **13,** 368–376.

Kunze, E. R., 1986: The mean and near-inertial velocity fields in a warm-core ring. *J. Phys. Oceanogr.*, **16,** 1444–1461.

Luyten, J. R., H. M. Stommel and C. I. Wunsch, 1985: A diagnostic study of the northern Atlantic subpolar gyre. *J. Phys. Oceanogr.*, **15,** 1344–1348.

Nof, D., 1981: On the beta-induced movements of isolated baroclinic eddies. *J. Phys. Oceanogr.*, **11,** 1662–1672.

——, 1983: On the migration of isolated eddies with application to Gulf Stream rings. *J. Mar. Res.*, **41,** 399–425.

——, 1985: Joint vortices, eastward propagating eddies and migratory Taylor columns. *J. Phys. Oceanogr.*, **15,** 1114–1137.

Olson, D. B., R. W. Schmitt, T. M. Joyce and M. E. Kennelly, 1985: A two-layer diagnostic model of the long-term physical evolution of warm-core ring 82B. *J. Geophys. Res.*, **90,** 8813–8822.

Pedlosky, J., 1986: The buoyancy and wind-driven ventilated thermocline. *J. Phys. Oceanogr.*, **16,** 1077–1087.

Schmitt, R. W., and D. B. Olson, 1985: Wintertime convection in warm core rings: Thermocline ventilation and the formation of mesoscale lenses. *J. Geophys. Res.*, **90,** 8823–8838.